Measurement of the thermal cycle in the base metal heat affected zone of cast ATI®718PlusTM during manual multi-pass TIG welding

Available online at www.sciencedirect.com

ScienceDirect

Procedia Manufacturing 25 (2018) 443–449

Procedia MANUFACTURING

www.elsevier.com/locate/procedia

8th Swedish Production Symposium, SPS 2018, 16-18 May 2018, Stockholm, Sweden

Measurement of the thermal cycle in the base metal heat affected zone of cast ATI®718Plus™ during manual multi-pass TIG welding

Fabian Hanning[a]*, Kjell Hurtig[b], Joel Andersson[b]

[a]*Department of Industrial and Materials Science, Chalmers University of Technology, 41296 Gothenburg, Sweden*
[b]*Department of Engineering Science, University West, Gustava Melins Gata 2, 46132 Trollhättan, Sweden*

Abstract

This paper presents a method to acquire thermal data in the base metal heat affected zone (HAZ) during manual multi-pass TIG welding of ATI®718Plus™, representing conditions close to an actual repair welding operation. Thermocouples were mounted in different locations along side walls of linear grooves to record temperature data. The thermal cycling was found to be largely independent of location within the HAZ. The recorded temperatures were below the incipient laves melting temperature, indicating that the current test setup requires optimisation to study HAZ liquation. Based on the results of this study, a modified thermocouple mounting technique is proposed.

Peer-review under responsibility of the scientific committee of the 8th Swedish Production Symposium.

Keywords: Nickel-based superalloys; Welding; Temperature measurement

1. Introduction

ATI®718Plus™ has been developed as a successor for Alloy 718, allowing an increase in maximum service temperature of about 50°C [1]. Originally developed as a wrought alloy, the material is now also available in cast form [2]. To be applicable for structural applications in the aerospace industry an alloy is required to be weldable since large structural components are often manufactured out of smaller wrought and cast parts [3]. Examples for the application of ATI®718Plus™ are compressor discs and low pressure turbine casings.

* Corresponding author. Tel.: +46-520-223-379.
E-mail address: fabian.hanning@chalmers.se

2351-9789
Peer-review under responsibility of the scientific committee of the 8th Swedish Production Symposium.
10.1016/j.promfg.2018.06.115

Table 1. Chemical composition of ATI®718Plus™ in wt.-%.

Ni	Cr	Co	Mo	Ti	Al	Fe	Mn	Si	C	B	Nb	W
Bal	20.72	8.34	2.71	0.75	1.50	9.31	0.01	0.04	0.05	0.005	6.02	1.00

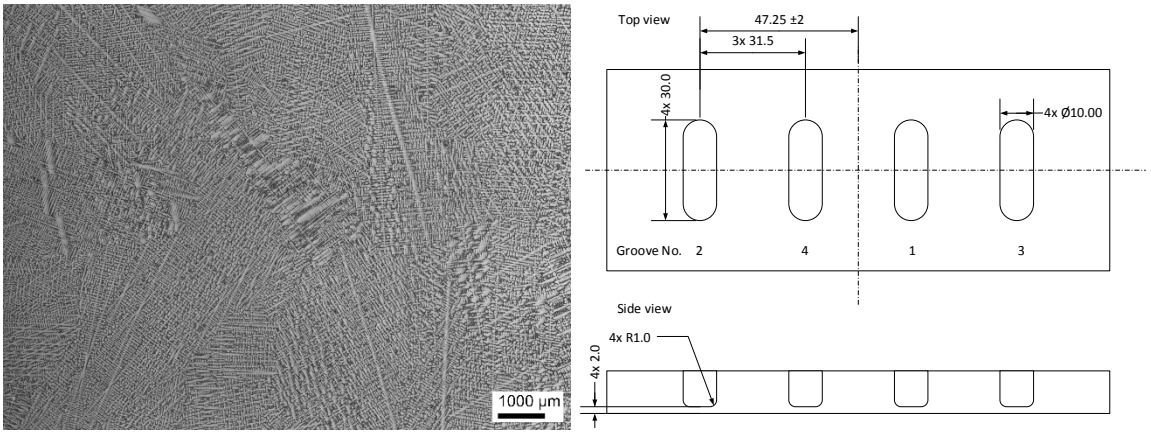

Fig. 1. (a) Microstructure of the cast plate (b) Dimensions and positioning of the welding grooves.

Both during the manufacturing process and in service it is often necessary to repair parts, which is economically more feasible than complete replacement. The commonly used method is repair welding, carried out manually by experienced welders using tungsten inert gas (TIG) welding. Such an operation can be performed on both cast and wrought parts and usually requires the removal of damaged sections and the subsequent joining or filling with weld deposits. The welding performance of cast ATI®718Plus™ as a function of base material thermal history has been investigated in previous studies [4,5]. To provide further insight in ongoing mechanisms and to relate microstructural changes in the base metal heat affected zone (HAZ) to the thermal cycle superimposed by the welding operation, it is necessary to acquire thermal data during the welding operation. This study hence aims to develop a method to mount thermocouples in the base metal HAZ in close vicinity to the fusion line to provide in-situ temperature data for a repair welding operation.

2. Experimental

Cast plates of ATI®718Plus™ with the dimensions of 150x60x12.7 mm have been investigated. The chemical composition given in Table 1 has been used with the material being in the as cast condition with an average hardness of 415 ± 5HV0.5 and grain size of 1300 ± 300µm. The microstructure is showing typical dendritic microstructure with Nb-rich precipitates in the interdendridic areas (cf. Fig. 1 a). While in practice such a material is usually homogenized, a previous study found that as cast microstructures are more resistant to HAZ liquation cracking [5], hence the choice of material condition for this investigation.

Four linear grooves with the dimensions 30x10x10 mm, a side radius of 5 mm and a bottom radius of 1 mm have been machined into the plate, together with holes for thermocouples drilled into the backside. The schematic drawing is shown in Fig. 1 b. The positioning of thermocouples along the sidewall of the grooves was chosen such that the thermal history of base metal HAZ could be studied as a function of weld layer deposition. On each side of the groove one thermocouple was placed at 25, 50 and 75% relative to the height of the groove, respectively. The position of the outer 2 thermocouples was reversed on one side of the groove, as indicated in Fig. 2 a.

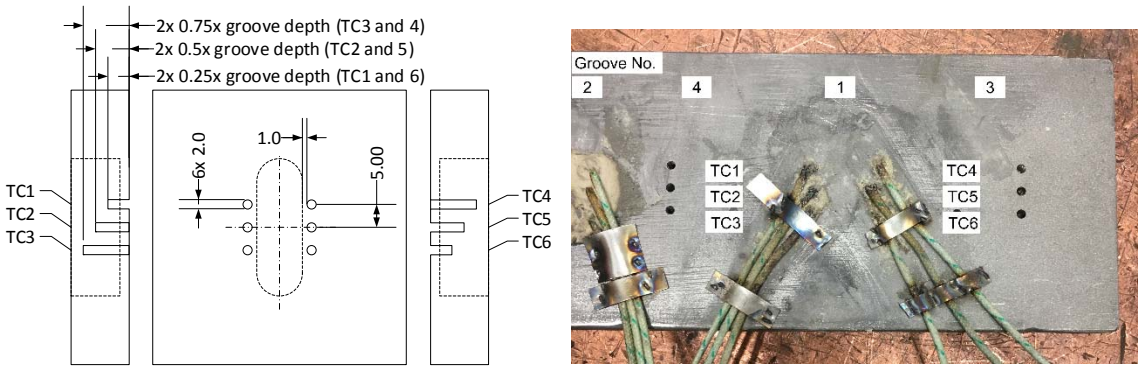

Fig. 2. (a) Dimensions and positions of holes for thermocouple placement; (b) Groove 1 with attached thermocouples TC1-6.

To achieve a stable mounting of the thermocouples within the holes, they were fixed using Omegabond® OB-400 high temperature, heat conductive cement. Movement has further been restricted by thin metal plates tack-welded onto the back of the cast plate. Type-K thermocouples with a diameter of 0.25 mm have been used in conjunction with a National Instruments NI cDAQ-9172 data logger, using a sampling rate of 10Hz.The complete setup is exemplarily shown in Fig. 2 b, with the numbers of the grooves indicating the order they have been welded. Since the placement of thermocouples on the backside of the plate required more space than the distance between two grooves allowed, the grooves have been filled in two consecutive operations (1-2 and 3-4).

The welding has been carried out manually by an experienced welder using TIG welding with argon as shielding gas and filler wire with matching chemistry. A 20wt.-% thorium (WT-20) tungsten electrode has been used with a shielding gas flow of 15l/min together with a 20 mm nozzle. The welding current was set to 140A and was temporarily adjusted by the welder if required during the process (e.g. start/stop location). A large electrode stick-out has been used to be able to reach the bottom of the grooves. The welding included a root pass to create a smoother bottom radius, followed by filling the grooves lengthwise, approximately covering half the width of a groove per pass. The plate was cooled with compressed air until an inter-pass temperature of approx. 200°C was reached. The following layer was started at the previous stop location and was then following the groove wall on the opposite site (i.e. the groove was filled in a spiral motion, with interruptions every half turn).

For visual inspection after the welding 3 cross sections have been prepared for each welded groove. They were positioned such that each of them intersected two thermocouple locations (one on each side of the groove). All samples have after cutting been mounted in hot mounting resin, followed by manual grinding to reach the desired cross section location. After automatic polishing the samples then have been electrolytically etched in 10wt.-% oxalic acid at 3V DC for 3-5s and visually inspected using a stereo and light optical microscope.

3. Results and discussion

The relative positioning of the thermocouples with respect to the weld is shown exemplarily in Fig. 3 for TC1 and 4 in groove 4, with the original groove location indicated by the dashed line. Due to the manual welding process the distance of the thermocouples to the fusion line is not the same for all placements. While the horizontal fusion line distance could be determined from the cross sections, this measurement would only be useful if the position of the weld torch could be correlated to the temperature recordings. The possibility of hitting the side wall with the arc during the deposition of a layer further below in the groove could explain why no direct correlation between maximum recorded temperature and layer count from the cross sections has been found. Re-melting during subsequent layer deposition furthermore makes a clear judgement difficult and unreliable. The horizontal distance to the fusion line has hence not been used for further evaluation and a more statistical approach is followed instead.

Table 2. Highest recorded temperature and time between 600 and 900°C per thermocouple location.

Groove	Thermocouple	Maximum temperature [°C]	Time between 600 and 900°C [s]
1	TC1	1254	48
	TC2	1105	93
	TC3	883	54
	TC4	984	59
	TC5	1071	79
	TC6	987	77
2	TC1	883	77
	TC2	932	92
	TC3	927	62
	TC4	972	89
	TC5	976	129
	TC6	988	84
3	TC1	912	55
	TC2	718	51
	TC3	936	59
	TC4	1159	105
	TC5	976	57
	TC6	1053	89
4	TC1	854	55
	TC2	837	61
	TC3	925	74
	TC4	1053	88
	TC5	1054	96
	TC6	884	54

Table 2 shows the highest recorded temperature and the accumulated time between 600 and 900°C for the complete welding operation. The latter represents time spend in the temperature range where precipitation of hardening phases such as gamma prime and gamma double prime occur and should therefore provide an indication for microstructural changes. The exposure time varies between 48 and 129 seconds, with an average time of 74 seconds. The peaks recorded during each weld pass reach lower values as more welding layers are deposited. Large scatter is present between the different thermocouples and a pattern could neither be identified when thermocouples were analysed based on the groove they were mounted at nor if grouped by their position along the groove side walls. The cause for the widely scattered temperature data has to be seen in the not precisely controllable workflow of manual welding. Furthermore, the different locations of the thermocouples and hence different distance to the weld torch at a given time during layer deposition contributed to the difference in temperature data.

Thermal cycles recorded at position 1 and 6 (25% of groove height, 1.34 and 1.37mm horizontal distance from fusion line, respectively) are exemplarily shown for groove 2 in Fig. 4. All temperature recordings show diffuse (i.e. not continuously cycling as during linear torch movement) thermal cycling in the beginning resulting from the deposition of a root bead in the grooves, as indicated in the figure. Peak analysis revealed that the maximum temperature rarely exceeded 1000°C. For groove 1 the temperature maxima were recorded during root pass deposition, while for groove 3 and 4 the maximum temperature was reached during the first 2 weld passes after the root bead had been deposited. No thermocouple in groove 2 recorded values exceeding 1000°C.

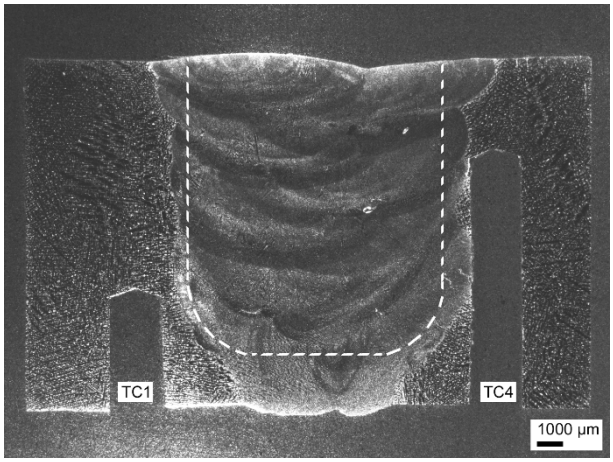

Fig. 3. Cross section of groove 4 showing the position of TC1 and 4 relative to the weld. Original groove position indicated by dashed line.

Cast Nb-bearing superalloys contain large amounts of laves phase due to Nb segregation in the melt. With the laves phase being a compound with significantly lower melting point than the matrix, the formation of liquid has to be expected in the material if the temperature is higher than the incipient laves melting temperature. For ATI®718Plus™, the incipient laves melting temperature is 1160°C [4], indicating that the thermocouples were mounted too far away from the groove side walls. The applied method was hence not capable of recording thermal data close enough to the fusion line to cover local melting. The general thermal cycling present during the repair welding operation could however be detected. The low repeatability and widely scattered data shows that the temperature cycle and experienced peak temperatures for a given location in the base metal HAZ largely depend on the welder that carries out the repair operation. It has to be pointed out that the groove geometry used in this investigation is a rather extreme one and the absence of a wide bottom radius, combined with the high welding current lead to difficult welding conditions.

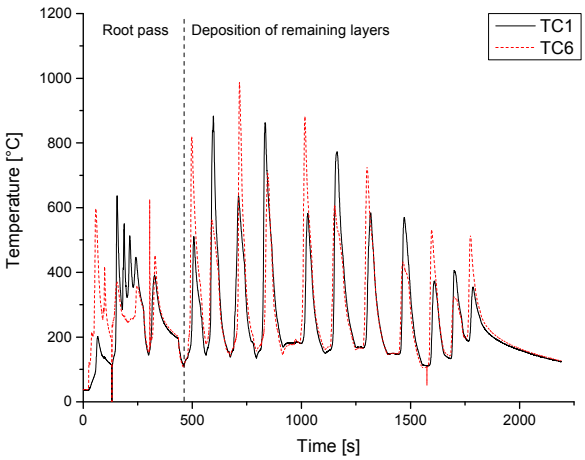

Fig. 4. Thermal profile recorded for TC1 and 6 (25% of groove height) at groove 2

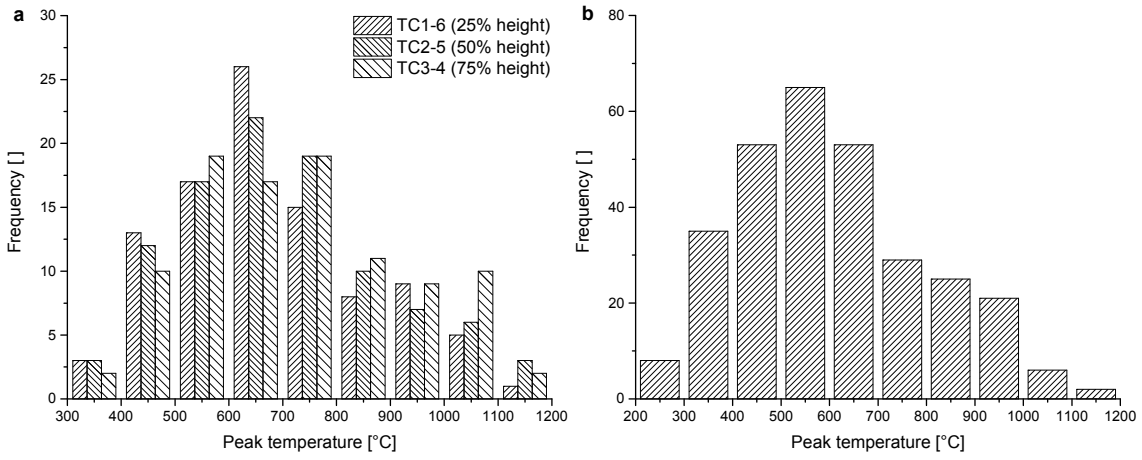

Fig. 5. Distribution of peak temperature during welding (a) grouped by position relative to groove height, (b) all thermocouples combined.

While it is not necessary to represent hard-to-weld conditions for recording thermal cycles, this study was aimed to provide additional temperature data for a previously carried out repair welding study [5] by using identical welding conditions. The frequency of observed peak temperatures during the complete welding operation is shown in Fig 5 a for thermocouples grouped by their location along the groove side walls. The small difference as compared to the distribution considering all thermocouples (Fig. 5 b) indicates that the location alongside the groove side walls has a very limited influence on the thermal cycle. The use of averaged values for exposure time should hence give a reasonable indication for the exposure time that could be expected for comparable repair welding operations. However, to be useful to explain HAZ liquation cracks commonly observed in the base metal HAZ, temperature data recorded more closely to the fusion line is necessary. With the used thermocouple placement it is not possible to obtain such data in a reliable way.

Based on the mostly location independent thermal cycling that has been observed in this study, a different thermocouple placement is proposed. Instead of mounting thermocouples at different locations along the welding groove, a placement perpendicular to the groove could mitigate the problem of relating torch position and recorded temperature. Fig. 6 shows such an alternative placement, where thermocouples are spot welded in defined distances to the groove side wall. Without the requirement of a minimum hole diameter, the distance to the fusion line could be reduced significantly. As indicated in the figure, placing the thermocouples in small v-grooves should enable putting the plates back together for the welding process. With such a thermocouples placement temperature data could be provided from different positions within the HAZ, starting close to the fusion line. A change in heat dissipation due to the cross sectioning of the welding groove has however to be taken into account.

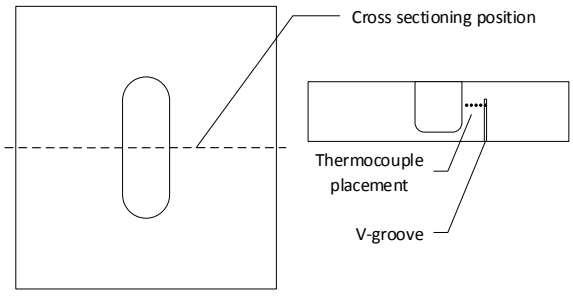

Fig. 6. Schematic visualization of the thermocouple placement proposed for further studies.

4. Conclusions

The thermal cycle during manual multi pass repair welding operations has been measured via thermocouples placed along the side walls of linear welding grooves. With thermocouple positioning via holes drilled into the back of the base metal plate it was not possible to get thermal data at locations close to the fusion line where the local solidus temperature is exceeded. The exposure time in the temperature range between 600 and 900°C was largely location independent, resulting from the variability of the manual welding process. The obtained data provides the basis for further investigations creating HAZ microstructures via controlled thermal cycling. A different thermocouple mounting technique has been proposed to avoid the shortcomings of the present study.

Acknowledgements

The support by the Consortium Materials Technology for Thermal Energy Processes (KME) through funding from Swedish Energy Agency and GKN Aerospace Sweden AB is highly appreciated. The authors sincerely acknowledge Andreas Lindberg and Jerry Isoaho from GKN Aerospace Sweden AB for the help with preparing the plates and carrying out the repair welding operation.

References

[1] W.D. Cao, R. Kennedy, Role of Chemistry in 718-Type Alloys - Allvac 718Plus Development, in: Proc. 10th Int. Symp. Superalloys, 2004. http://www.tms.org/superalloys/10.7449/2004/Superalloys_2004_91_99.pdf (accessed March 17, 2015).

[2] B. Peterson, D. Frias, D. Brayshaw, R. Helmink, S. Oppenheimer, E. Ott, R. Benn, M. Uchic, On the Development of Cast ATI 718Plus® Alloy for Structural Gas Turbine Engine Components, in: Superalloys 2014 Conf. TMS, 2012.

[3] G. Sjöberg, Casting Superalloys For Structural Applications, in: 7th Int. Symp. Superalloy 718 Deriv., The Minerals, Metals & Materials Society, 2010: pp. 117–130. doi:10.1002/9781118495223.ch8.

[4] J. Andersson, G. Sjöberg, H. Hänninen, Metallurgical Response of Electron Beam Welded Allvac 718Plus™, in: Hot Crack. Phenom. Welds III, Springer Berlin Heidelberg, 2011: pp. 415–429.

[5] F. Hanning, Andersson, Joel, The influence of base metal microstructure on weld cracking in manually GTA repair welded cast ATI 718Plus®, in: Proc. 2018 Superalloy 718 Deriv. Energy Aerosp. Ind. Appl., The Minerals, Metals & Materials Society, Pittsburgh, USA, 2018: p. submitted manuscript.